Effect of annealing on structural and optical properties of lead tungstate microcrystals*

Pang Hua-Feng(庞华锋)[a)], Li Zhi-Jie(李志杰)[a)], Xiang Xia(向 霞)[a)b)], Zhang Chun-Lai(章春来)[a)], Fu Yong-Qing(傅永庆)[c)], and Zu Xiao-Tao(祖小涛)[a)b)†]

[a)] *Department of Applied Physics, University of Electronic Science and Technology of China, Chengdu* 610054, *China*

[b)] *International Center for Material Physics, Chinese Academy of Sciences, Shenyang* 110015, *China*

[c)] *Thin Film Centre, Scottish Union of Physics Alliance, University of the West of Scotland, Paisley, PA1 2BE, UK*

(Received 27 March 2011; revised manuscript received 19 June 2011)

Shuttle-like lead tungstate ($PbWO_4$) microcrystals are synthesized at room temperature using the precipitation method with the cetyltrimethyl ammonium bromide. Results from both the X-ray diffraction and the scanning electron microscopy show that the lattice distortions of the $PbWO_4$ microcrystals are reduced significantly when the annealing temperature is increased to 873 K. The result from the ultraviolet-visible diffuse reflectance spectroscopy shows that the exciton absorption appears in the sample annealed at 673 K. The self-trapped exciton luminescence due to the Jahn–Teller effect is also observed in the blue band. The interstitial oxygen ions in the $WO_4{}^{2-}$ groups are mainly resposible for the enhancement effect of the green luminescence of the annealed samples. The above results are supported by the spectrum analysis of the as-grown and the post-annealed samples using the X-ray photoelectron spectroscopy.

Keywords: $PbWO_4$ microcrystal, annealing, defects, photoluminescence

PACS: 61.72.Cc, 71.55.Ht, 71.70.Ej **DOI:** 10.1088/1674-1056/20/11/116104

1. Introduction

As an important scintillating medium, the $PbWO_4$ crystal has been used in the high-energy physics, e.g., as a new-generation crystal calorimeter in the Large Hadron Collider project.[1,2] As a good imaging sensor, it is also used for the positron emission computed tomography in the medical diagnostics.[3] The bulk $PbWO_4$ crystal normally has high density, fast luminescence and good radiation tolerance, whereas for the $PbWO_4$ nano- and microcrystals, their scintillation and optical properties depend on their crystallographic structures and specific shapes. The scintillating mechanism of the $PbWO_4$ crystal is affected by the optical absorption in the UV and the blue spectral bands created from the colour centres of the defects.[4,5] The controlled synthesis of the $PbWO_4$ nano- and microcrystals with well-defined shapes and microstructures becomes one of the principle routes to the investigation of the properties of different defects.[6−8]

The post annealing is often used to improve the quality of the as-prepared $PbWO_4$ crystals. The interior stress and lots of defects in the $PbWO_4$ crystals can be effectively removed by the post annealing. Much attention has been paid to the study of the effects of annealing on the scintillation and the optical properties of the $PbWO_4$ crystallites.[9−12] After investigating the annealed $PbWO_4$ crystallites in air and in vacuum, Nikl *et al.*[13] concluded that the UV band at 350 nm and the blue band at 420 nm in the absorption spectra originated from the Pb^{3+} and the O^- hole centres, respectively. Han *et al.*[14] showed that the post-annealing treatments of the $PbWO_4$ crystallites above 1013 K in air could annihilate the UV optical absorption band at 350 nm and they concluded that the conversion of the Pb^{3+} hole centres into the Pb^{4+} ions led to the annihilation of the 350 nm absorption band. However, there is still a huge controversy over the extrinsic origins of the scintillation and the optical properties of the annealed $PbWO_4$ crystals.

Recently, the $PbWO_4$ nano- and microcrystals

*Project supported by the Fundamental Research Funds for the Central Universities, China (Grant Nos. ZYGX2009J046 and ZYGX2009X007), the Sichuan Provincial Young Scientists Foundation, China (Grant No. 2010JQ0006), the Royal Society-Research Grant, UK (Grant No. RG090609), and the Royal Academy of Engineering-Research Exchanges with China and India Awards in UK.

†Corresponding author. E-mail: xtzu@uestc.edu.cn

© 2011 Chinese Physical Society and IOP Publishing Ltd

have been prepared through a wet chemical method by using the cetyltrimethyl ammonium bromide (CTAB) as the surfacant.[15−19] However, to our best knowledge, the effects of annealing on the structural and the optical properties of the wet-chemically prepared $PbWO_4$ microcrystals have not been reported yet. In this paper, a simple and direct precipitation method is used to synthesize the $PbWO_4$ microcrystals at room temperature and the microstructures, the optical properties and the chemical bindings of the as-grown and the annealed samples are analysed in detail.

2. Experiment

The analytical grade precursors used for the synthesis of the $PbWO_4$ microcrystals included the sodium tungstate ($Na_2WO_4{\cdot}2H_2O$, Tianjin City Rgent Chemicals Co.), the CTAB ($C_{16}H_{33}(CH_3)_3NBr$, Chengdu Kelong Chemical Reagent Co.) and the lead acetate ($Pb(CH_3COO)_2{\cdot}3H_2O$, Tianjin Kermel Chemical Reagent Co.). In a typical process to synthesize the $PbWO_4$ microcrystals by using the co-precipitation method at room temperature, a sodium tungstate solution was formed by dissolving 3.298 g sodium tungstate into 30 ml de-ionized water in a beaker. About 0.5 g CTAB was added into the above solution and the solution was continuously stirred until it became transparent. A lead acetate solution was prepared in another beaker by mixing 3.793 g lead acetate and 30 ml de-ionized water. When the aqueous lead acetate solution was dripped slowly into the former prepared solution under magnetic stirring at room temperature, some white precipitates were formed. After leaving the mixed solution for 24 h, the white precipitates were filtered, washed with the de-ionized water several times and dried at 373 K in air for 5 h. Some of the as-grown $PbWO_4$ powders were annealed at 673 K or 873 K for 3 h.

The crystalline structure of the powders was characterized by the X-ray diffraction (XRD) using a Dandong Fangyuan X-ray diffractometer (DX-2700) equipped with the copper Kα radiation ($\lambda = 15418$ Å) and a graphite monochromator. The morphologies of the powders were observed using a scanning electron microscope (SEM, JSM-5900LV, JEOL Ltd.). The ultraviolet-visible (UV-Vis) diffuse reflectance spectroscopy (UV-Vis DRS) was obtained using an UV-Vis spectrophotometer (Shimadzu UV2550-PC) equipped with an integrating sphere and a $BaSO_4$ reference. The photoluminescence (PL) spectrum analysis was carried out using a fluorescence spectrometer (Shimadzu rf-5301PC) at room temperature. The X-ray photoelectron spectra (XPS) were obtained using an electron spectrometer (XSAM800, Kratos Ltd.) equipped with an Al Kα X-ray source (1486.6 eV) under a background pressure of 2×10^{-7} Pa. The analyzer mode was fixed to the analyzer transmission (FAT). All the binding energies were calibrated against the C 1s line (284.6 eV) from the adventitious carbon on the samples.

3. Results

3.1. Crystalline structure and morphology

The XRD patterns of the $PbWO_4$ microcrystals are shown in Fig. 1(a). All the diffraction peaks can be indexed to a pure tetragonal stolzite phase of the $PbWO_4$ with cell parameters of $a = 5.4450$ Å and $c = 12.0495$ Å (JCPDS card No. 85-1857). In the XRD patterns, the diffraction peaks of (112) and (200) are much stronger than the other ones. The XRD results confirm that the as-prepared samples are well crystallized. Several peaks in the patterns of the annealed samples are quite different from those of the as-grown samples. There are about 0.1° deviations from the JCPDS card data of the $PbWO_4$ crystal at the (112), (004), (200) and (220) peaks of the as-grown samples. It shows that there is a certain distortion in the crystal cell of the as-grown sample.

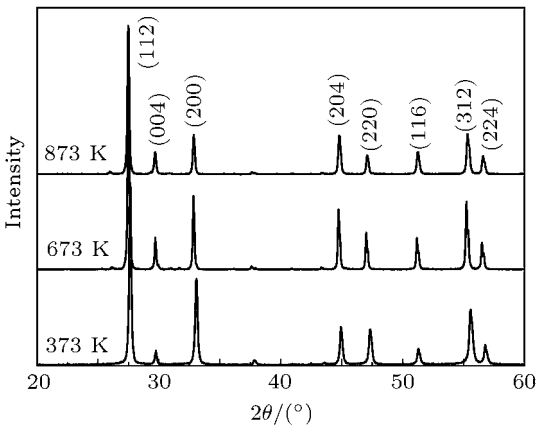


Fig. 1. XRD patterns of the samples heat-treated at 373 K, 673 K and 873 K.

The average lattice constants of the three XRD patterns are calculated by using the Jade 5 software. The lattice constants of the $PbWO_4$ crystals

are $a_1 = 5.4010$ Å, $c_1 = 12.0970$ Å; $a_2 = 5.4416$ Å, $c_2 = 12.0802$ Å; and $a_3 = 5.4459$ Å, $c_3 = 12.0678$ Å for the samples heat-treated at 373 K, 673 K and 873 K, respectively. It is clear that the lattice constants are near to those corresponding to the standard XRD pattern in the JCPDS card. The lattice distortions of the as-grown $PbWO_4$ microcrystals are possibly caused by the preferential growth along a certain crystallographic direction.

The SEM images of the samples are presented in Figs. 2(a)–2(c). The typical morphology of the $PbWO_4$ microcrystal exhibits a shuttle-like shape as shown in Fig. 2(a). The lengths of the microcrystal particles range from 2 μm to 10 μm. The trifurcate and the flower-like morphologies are also observed in Fig. 2(a). Those morphologies are different from the dentrite, the spindle-like, or the trunk shapes synthesized using the surfactant CTAB.[14,16,18] It is concluded that the morphology of the $PbWO_4$ crystal is very sensitive to the concentration of the CTAB. The shape of the $PbWO_4$ microcrystal depends on the relatively specific surface energy related to the facets of the small primary particles.[20] At the initial stage of the crystallization, the $PbWO_4$ nuclei aggregate into small primary particles, which serve as the $PbWO_4$ crystal seeds. The adsorption and the desorption of the CTAB polar groups on some facets of the crystal seeds with different velocities result in the highly anisotropic growth. Then, the crystal seeds grow preferentially in a certain direction without the restrictions of the adsorption from the CTAB polar groups to form the different structures. The shuttle-like $PbWO_4$ crystals annealed at 673 K change into the rod-like morphology with spherical heads, as shown in Fig. 2(b). The rod-like morphology conforms with the above analysis of the lattice constants based on the XRD patterns. The peanut-like or the spherical structure of the $PbWO_4$ crystals shown in Fig. 2(c) can be observed when the temperature is increased to 873 K. The intensity of the lattice relaxation becomes stronger with the annealing temperature increasing. The grain boundaries could be extended and inosculated at the points where no defects exist. Therefore, the grains of the annealed samples grow much bigger than those of the as-grown samples and the $PbWO_4$ microcrystals are changed into different morphologies after the annealing.

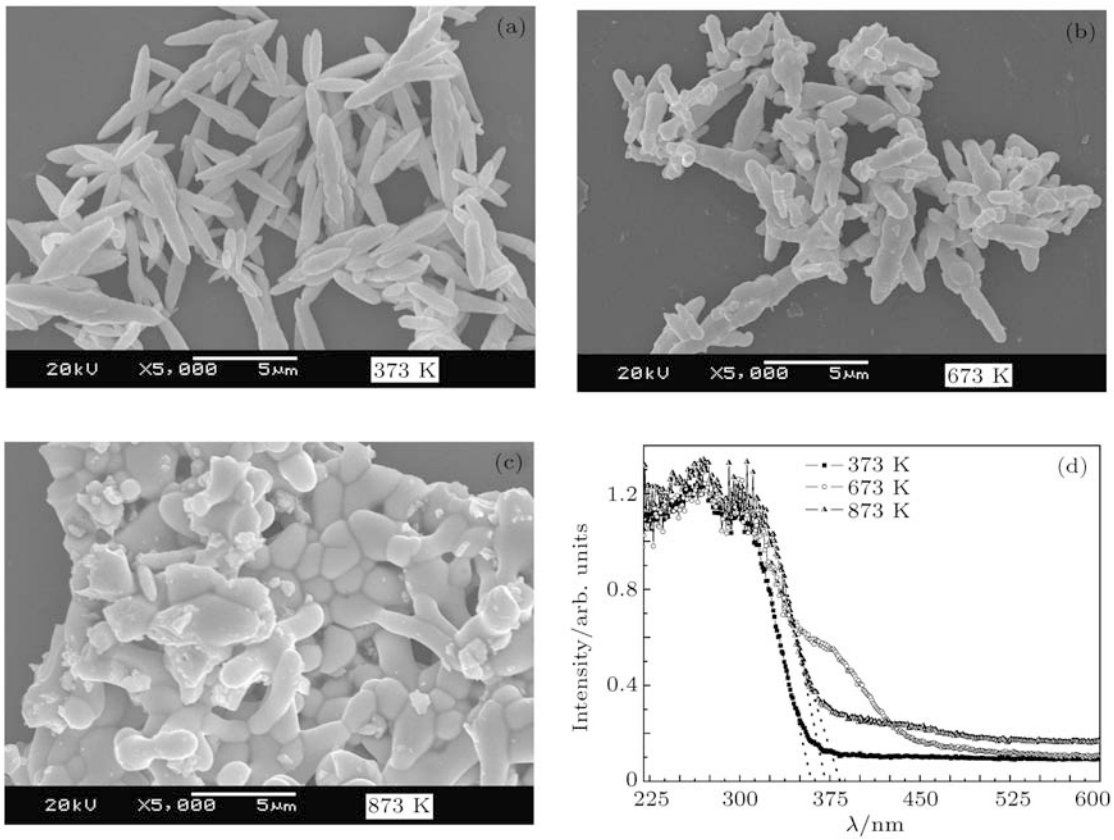


Fig. 2. Morphologies of the samples heat-treated at 373 K (a), 673 K (b), and 873 K (c). (d) UV-vis absorption spectra of $PbWO_4$ microcrystals.

3.2. Effect of annealing on UV-Vis DRS

The UV-Vis absorption spectra of the $PbWO_4$ microcrystals are presented in Fig. 2(d). The broad band between 225 nm and 350 nm is attributed to the charge transfer transition of the WO_4^{2-} anion. The absorption edge of each sample is determined by drawing a tangential line on the absorption spectrum. The value of the absorption edge of the as-grown sample is 358 nm and the band gap energy corresponds to 3.47 eV. The wavelengths of the absorption edges are 382 nm (3.25 eV) and 373 nm (3.33 eV) for the samples annealed at 673 K and 873 K, respectively. The range of the absorption edge is consistent with that reported by Nikl *et al.*[13] The absorption spectrum of the sample annealed at 673 K shows a shoulder band ranging from 350 nm to 425 nm near the absorption edge, which is possibly due to the absorption of the self-trapped exciton (STE) in the WO_4^{2-} groups. The red shift of the absorption edge from 358 nm to 373 nm is related to the transforming structure caused by the annealing. The absorption band in the range from 350 nm to 425 nm increases first and then decreases significantly with the increase of the temperature. A similar phenomena have been reported in the literature.[9,13]

3.3. Effect of annealing on photoluminescence

The room-temperature PL spectra of the $PbWO_4$ microcrystals are shown in Fig. 3. Each emission spectrum of the samples consists of an ultraviolet band and a blue band. As shown in Fig. 3(a), the ultraviolet band has a broad peak around 364 nm under the excitation at the wavelength of 250 nm. Because most of the oxygen defects on the surfaces of the microcrystals gradually disappear, the intensity of the ultraviolet band of the annealed sample become much weaker than that of the as-grown sample when the annealing temperature is increased to 873 K. The blue wide band has a main peak at 425 nm, which can be deconvoluted into three Gaussian peaks centered at 402 nm, 420 nm and 452 nm. The energy separations between the Gaussian peaks are calculated to be $\Delta_1 = 0.14$ eV between the 402 nm and the 420 nm peaks and $\Delta_2 = 0.21$ eV between the 420 nm and the 452 nm peaks. The obtained triplet Gaussian peaks accord with the data in the literature obtained by using the time-resolved luminescence.[21−23] The triplet peaks are also consistent with the blue emission band caculated by Bacci *et al.*,[24,25] who have developed a general theory for those tetrahedral complexes.

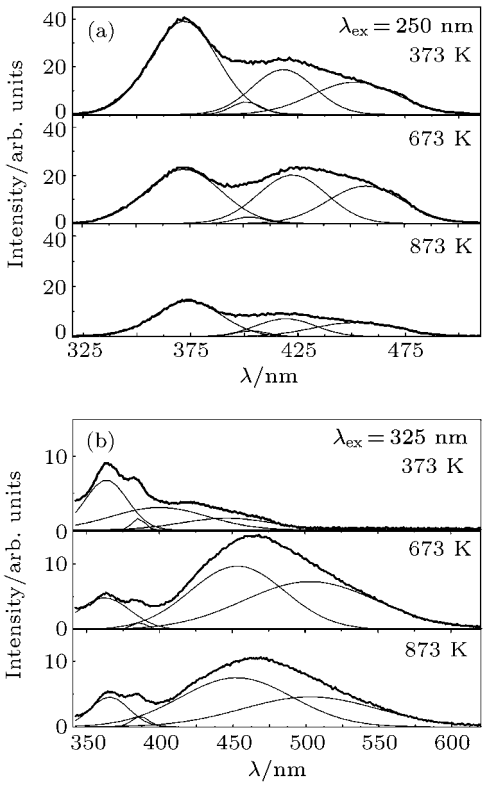


Fig. 3. Emission spectra of the $PbWO_4$ microcrystals excited at (a) 250 nm and(b) 325 nm.

The intrinsic blue luminescence at 425 nm is ascribed to the radiative recombination of the STE localized at the tetrahedral WO_4^{2-} complex anions.[26,27] The triplet peaks of the overlapping band originate from the transition of the excited states $^3T_2$ and $^3T_1$ to the ground state $^1A_1$. Due to the Jahn–Teller effect, the slight distortion lowers the tetrahedral symmetry from T_d to C_{3v}. Therefore, the $^3T_2$ state splits into the $^3A_1$ and the ^3E states. The $^3T_1$ state also splits into the $^3A_2$ and the ^3E states.

The intensity of the blue band becomes stronger for the sample annealed at 673 K and is obviously much weaker for the sample annealed at 873 K. This dependence on the annealing temperature indicates that the oxygen defects have an influence on the radiative recombination of the STE. Lots of oxygen defects are filled by the oxygen atoms from air when the sample is annealed at 673 K. Therefore, the Jahn–Teller effect is enhanced, because the length of the W–O bond and the angle of the O–W–O bond have been locally distorted. However, the effect is weakened after the crystal lattice relaxation, as in the crystals annealed at 873 K. The rapid decrease in the distor-

tion can be confirmed by the variation of the lattice constants of the $PbWO_4$ crystals.

The emission spectra excited at the wavelength of 325 nm are shown in Fig. 3(b). The ultraviolet band shows two peaks centred at 359 nm and 383 nm. The wide blue–green band ranging from 400 nm to 600 nm is dominated by the main blue luminescence at 469 nm for the annealed samples, which differs from that of the as-grown sample. The blue–green band can be deconvoluted into two Gaussian peaks centred at 453 nm and 505 nm. The green light emission at 505 nm in the overlapping emission band is strongly enhanced for the sample annealed at 673 K and is decreased for the sample annealed at 873 K. It indicates that the annealing in air is conducible to the green light emission. The interstitial oxygen ions in the WO_4^{2-} anions are considered to be the origin of the green light emission. The interstitial oxygen ions move to the inner-site positions when the oxygen concentration of the $PbWO_4$ crystal is lower than those annealed in air at 673 K and 873 K. Therefore, the interstitial oxygen ions form the WO_4+O_i^{2-} centres, which account for the transition of the green emission.[28,29] The emission spectrum excited at 325 nm is quite different from that excited at 250 nm. The difference could be interpreted by the fact that the transitions take place only when the energy of the photon meets the transition rule of the colour centre.

3.4. Effect of annealing on XPS spectrum

Figure 4 shows the XPS spectra of Pb 4f, W 4f and O 1s for the as-grown and the heat treated samples. Each spectrum has subtracted the Shirley background and the deconvolution of the peaks is based on 80% Gaussian and 20% Lorentzian.

The molar ratios of the three elements, i.e., Pb, W and O, are calculated to be 1.48:1:3.82 for the as-grown sample, 2.03:1:4.21 for the sample annealed at 673 K and 1.73:1:4.18 for the sample annealed at 873 K. It shows that the Pb atoms are excess on the surfaces of the samples, which can be used to explain that the CTAB molecules could be selectively adsorbed on the surface through the Pb–O bonding. The molar percentage of the element Pb increases after the annealing probably due to the decomposition of the CTAB polar groups.

The XPS spectra of Pb 4f are deconvoluted into two doublets as shown in Fig. 4(a). The first doublet peaks of the as-grown sample are at the binding energies of 138.04 eV (for Pb $4f_{7/2}$) and 142.99 eV (for Pb $4f_{5/2}$), which can be assigned to the Pb–Br binding on the surface caused by the CTAB.[30] The spin-orbital splitting of the Pb 4f orbital causes the energy separation of 4.95 eV. The second doublet peaks are located at 139.02 eV (for Pb $4f_{7/2}$) and 143.88 eV (for Pb $4f_{5/2}$), which are attributed to the Pb–O binding.[31,32] The intensity ratios of the two chemical states are 46.33% and 53.67%, respectively. The ratio of the latter chemical state increases to 58.36% for the samples annealed at 673 K and to 62.39% for the samples annealed at 873 K. This indicates that the surface oxygen can be effectively compensated by the annealing.

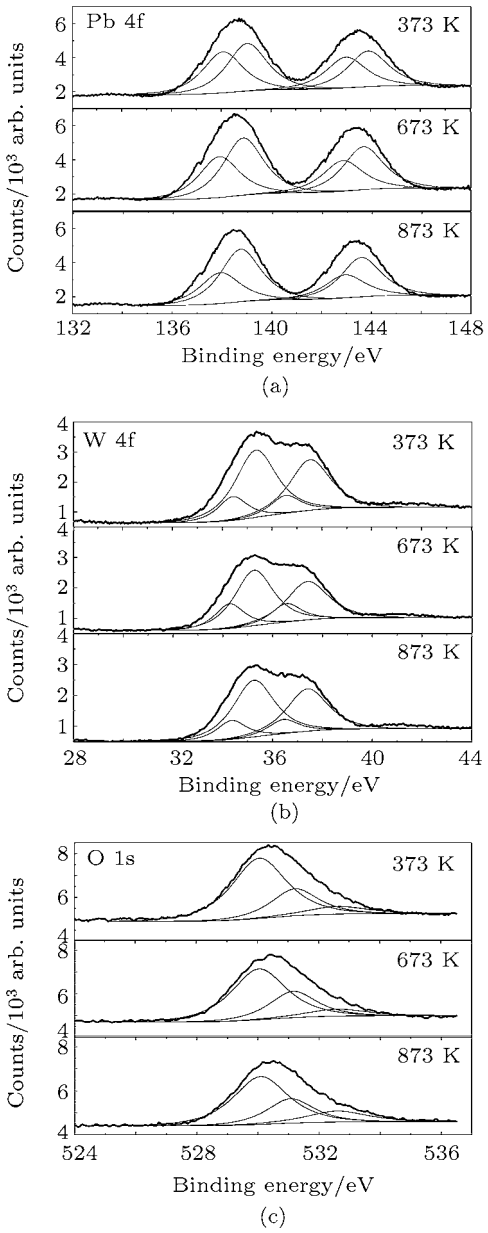


Fig. 4. XPS spectra of (a) Pb 4f, (b) W 4f, and (c) O 1s for $PbWO_4$ microcrystals.

Each W 4f XPS spectrum has a main peak and a shoulder peak, which indicates that there are W^{5+} oxidazition states besides the W^{6+} oxidizition states in the microcrystals.[33,34] The deconvolution curve fitting is shown in Fig. 4(b). The first doublet peaks of the W^{6+} ions are at 35.33 eV (for W $4f_{7/2}$) and 37.50 eV (for W $4f_{5/2}$). The energy separation is 2.17 eV due to the spin-orbital splitting of W 4f. The second doublet peaks of the W^{5+} ions are at binding energies of 34.40 eV (for W $4f_{7/2}$) and 36.52 eV (for the W $4f_{5/2}$). The calculated percentages of the W^{6+} and the W^{5+} ions are 79.7% and 20.3%, respectively. The percentage of W^{5+} is changed to 25.5% for the sample annealed at 673 K and to 19.3% for that annealed at 873 K. It suggests that the annealing cannot fully oxidize the microcrystals. Therefore, all the three samples have oxygen defects, which accords with the analysis of the peak at 365 nm in the PL spectrum.

In Fig. 4(c), the O 1s spectra are asymmetrical, which indicates the existence of oxygen in different chemical states. Each O 1s spectrum is deconvoluted into three components. The spectrum of the as-grown sample is deconvoluted into peaks centred at 530.05 eV (65.67%), 531.22 eV (25.23%) and 532.60 eV (9.1%). The main peak centred at 530.05 eV is considered to originate from O^{2-} in the stoichiometrical WO_4^{2-} structure. Although there are lots of oxygen defects, the peak at 531.22 eV appears only in the spectrum of the as-grown sample. Therefore, the peak at 531 eV should not be ascribed to the interstitial oxygen ions.[35] It is possibly due to the oxygen atoms in the Pb–O or the W=O bond.[31,33] The peak at 532.30 eV can be assigned to the oxygen in the adsorbed oxygen molecules or the water molecules.

The O 1s XPS peaks of the sample annealed at 673 K are located at 530.03 eV (62.79%), 531.15 eV (27.83%) and 532.59 eV (9.38%). The peaks of the sample annealed at 873 K are slightly shifted to 530.09 eV (59.26%), 531.07 eV (25.90%) and 532.59 eV (14.84%), respectively. The decrease of the intensity ratios of the main peaks indicates that the coordinate environment has been locally changed by the excess oxygen in the microcrystals, which means a new kind of interstitial oxygen atom must appear in the annealed samples. Therefore, it is certain that the interstitial oxygen atoms have an important influence on the XPS spectrum of the annealed sample. In addition, the adsorbed oxygen atoms on the surface of the annealed sample increase in intensity from 15.60% to 18.49%. However, the adsorbed oxygen atoms can be reduced obviously when the annealing temperature is increased to 1113 K.[33]

The above results of the XPS analysis have an intrinsic relation with the crystal structure. The calculated lattice constant c is decreased, while a is increased for the PWO_4 microcrystals, when the annealing temperature is increased to 873 K. The lattice constant c of the as-grown PWO_4 crystal is larger than that deduced from the standard XRD pattern in the JCPDS card due to the faster growth rate of a certain plane about the c axis. The results indicate that lots of oxygen defects appear in the microcrystals and the W/O mole ratio of 1:3.8 is larger than the stoichiometrical ratio of 1:4. When the PWO_4 microcrystals are annealed at 673 K, the surface oxygens adsorbed on the surface are locally coupled with the surface reaction and enter into the microcrystals. Then, the oxygen defects locally disappear via the nonhomogeneous diffusion of the oxygen atoms in the microcrystals. In addition, many oxygen atoms move into the interstitial sites of the WO_4^{2-} tetrahedron, because the concentration of the oxygen atoms is locally higher than the stoichiometrical one. The oxygen defects and the intersitial oxygen might coexist in the microcrystals based on the XPS analysis of the W and the O elements. As a result, the lattice distortion becomes weak and the lattice constant c is decreased. When the annealing temperature is increased to 873 K, the probability of the combinations between the oxygen defects and the diffused oxygens is increased to be larger than that of the crystals annealed at 673 K. The lattice constant c decreases, while it still deviates slightly from the lattice constant of 12.0495 Å, because it is impossible that the oxygen defects and the interstitial oxygen atoms can disappear completely in the tetrahedral WO_4^{2-} structure. Therefore, the concentration of the interstitial oxygen atoms decreases, which leads to the weaker green emission compared with that of the crystals annealed at 673 K.

4. Conclusion

Shuttle-like $PbWO_4$ microcrystals are synthesized at room temperature through the direct precipitation method assisted by the CTAB. The effects of the annealing on the structural and the optical properties are studied in detail. The XRD analysis reveals that the crystal lattice distortions of the samples are reduced

dramatically after the annealing at 873 K. The morphology of the annealed $PbWO_4$ microcrystal changes into the rod-like shape at 673 K and the peanut-like shape at 873 K. The STE luminescence due to the Jahn–Teller effect is observed in the blue band. The enhancement effect of the green band at 505 nm is observed in the emission spectrum with an excitation wavelength of 325 nm, which is due to the transitions of the interstitial oxygen ions in the WO_4+O_i^{2-} centre. The above results are supported by the XPS spectrum analysis.

References

[1] Lecoq P, Dafinei I, Auffray E, Schneegans M, Korzhik M V, Missevitch O V, Pavlenko V B, Fedorov A A, Annenkov A N, Kostylev V L and Ligun V D 1995 *Nucl. Instrum. Methods Phys. Res.* A **365** 291

[2] Zhu R Y, Ma D A, Newman H B, Woody C L, Kierstead J A, Stoll S P and Levy P W 1996 *Nucl. Instrum. Methods Phys. Res.* A **376** 319

[3] Kobayashi M, Usuki Y, Ishii M and Nikl M 2002 *Nucl. Instrum. Meth.* A **486** 170

[4] Feng X Q and Tong B T 2003 *Acta Phys. Sin.* **52** 2066 (in Chinese)

[5] Geng J, Lv Y, Lu D and Zhu J J 2006 *Nanotechnology* **17** 614

[6] Ryu J H, Yoon J W and Shim K B 2005 *Solid State Commun.* **133** 657

[7] Yang J, Lu C, Su H, Ma J, Cheng H and Qi L 2008 *Nanotechnology* **19** 035608

[8] Yu J G, Zhao X F, Liu S W, Li M, Mann S and Ng D H L 2007 *Appl. Phys.* A **87** 113

[9] Baccaroa S, Borgiab B, Cavallarib F, Ceciliaa A, Diemozb M, Festinesia A, Leonardib E, Lobkoc A, Longob E, Montecchia M, Organtinib G and Rapone B 1997 *J. Luminesc.* **72–74** 748

[10] Krasnikov A, Laguta V, Nikl M and Zazubovich S 2007 *J. Phys.: Condens. Matter* **19** 306202

[11] Bohacek P and Nikl M 2005 *Nucl. Instrum. Methods Phys. Res.* A 537 86

[12] Bohacek P, Solovieva N and Nikl M 2008 *IEEE Trans. Nucl. Sci.* **55** 1289

[13] Nikl M, Nitsch K, Baccaro S, Cecilia A, Montecchi M, Borgia B, Dafinei I, Diemoz M, Martini M, Rosetta E, Spinolo G, Vedda A, Kobayashi M, Ishii M, Usuki Y, Jarolimek O and Reiche P 1997 *J. Appl. Phys.* **82** 5758

[14] Han B, Feng X, Hu G, Zhang Y and Yin Z 1999 *J. Appl. Phys.* **86** 3571

[15] Zhou G, Wang S, Lu M, Xiu Z and Zhang H 2005 *Mater. Chem. Phys.* **93** 138

[16] Lei F, Yan B, Chen H H, Zhang Q and Zhao J T 2009 *Cryst. Growth Des.* **9** 3730

[17] Huo L and Chu Y 2006 *Mater. Lett.* **60** 2675

[18] Wang G and Wan G 2009 *J. Alloy Compd.* **484** 505

[19] Wang G Z and Hao C C 2009 *Mater. Res. Bull.* **44** 418

[20] George T, Joseph S, Sunny A T and Mathew S 2008 *J. Nanopart. Res.* **10** 567

[21] Itoh M and Sakurai T 2005 *Phys. Stat. Sol.* (b) **242** R52

[22] Itoh M and Sakurai T 2006 *Phys. Rev.* B **73** 235106

[23] Itoh M and Aoki T 2010 *J. Phys.: Condens. Matter* **22** 045503

[24] Bacci M, Porcinai S, Mihokova E, Nikl M and Polak K 2001 *Phys. Rev.* B **64** 104302

[25] Bacci M, Mihokova E and Schulman L S 2002 *Phys. Rev.* B **66** 132301

[26] Leonelli R and Brebner J L 1986 *Phys. Rev.* B **33** 8649

[27] Kobayashi M, Ishii M, Usuki Y and Yahagi H 1993 *Nucl. Instrum. Methods Phys. Res.* A **333** 429

[28] Shi C, Wei Y, Yang X, Zhou D, Guo C, Liao J and Tang H 2000 *Chem. Phys. Lett.* **328** 1

[29] Chen Y, Shi C and Hu G 2000 *J. Appl. Phys.* **87** 1503

[30] Wagner C D, Riggs W M, Davis L E, Moulder J F and Mullenberg G E 1992 *Handbook of X Ray Photoelectron Spectroscopy* (Minnesota: Perkin-Elmer Corporation) p. 160

[31] Yang Y, Taggart D K, Brown M A, Xiang C, Kung S C, Fan Y, Hemminger J C and Penner R M 2009 *ACSNANO* **3** 4144

[32] Gong W, Li J F, Chu X, Gui Z and Li L 2004 *Acta Mater.* **52** 2787

[33] Senthil W and Yong K 2007 *Nanotechnology* **18** 395604

[34] Phuruangrat A, Ham D J, Hong S J, Thongtema S and Lee J S 2010 *J. Mater. Chem.* **20** 1683

[35] Zhu W, Feng X, Wu Z and Man Z 2002 *Physica* B **324** 53